Published in Molecular and Cellular Neuroscience 25(4): 650-663, 2004

Parvalbumin-deficiency affects network properties resulting in increased susceptibility to epileptic seizures

B. Schwaller[1]*, I. V. Tetko[2], P. Tandon[3], D. C. Silveira[3], M. Vreugdenhil[4], T. Henzi[1], M.-C. Potier[5], M. R. Celio[1] and A.E.P. Villa[2,6]. [1] Division of Histology, Department of Medicine, University of Fribourg, CH-1705 Fribourg, Switzerland, [2] Laboratoire de Neuroheuristique, Institute of Physiology, University of Lausanne, Switzerland, [3]Dept. of Neurology, Children's Hospital and Harvard Medical School, Harvard Institute of Medicine, Boston, USA, [4]Dept. of Neurophysiology, Division of Neuroscience, Medical School, University of Birmingham, Edgbaston, Birmingham, U.K., [5]Laboratoire de Neurobiologie, CNRS UMR7637, ESPCI, Paris, France and [6]Laboratoire de Neurobiophysique, INSERM U318, Université "Joseph Fourier", Grenoble 1, France

Running title: Parvalbumin-deficiency and seizure susceptibility

* Correspondence to:

Dr. Beat Schwaller, Division of Histology Department of Medicine

University of Fribourg, Perolles, CH-1705 Fribourg, Switzerland

Tel: ++41 26 300 85 08 (Secr. 84 90) Fax: ++41 26 300 97 32

E-mail: Beat.Schwaller@unifr.ch

The manuscript contains 40 text pages, 6 figures and 2 tables.

Abstract

Networks of GABAergic interneurons are of utmost importance in generating and promoting synchronous activity and are involved in producing coherent oscillations. These neurons are characterized by their fast-spiking rate and by the expression of the Ca^{2+}-binding protein parvalbumin (PV). Alteration of their inhibitory activity has been proposed as a major mechanism leading to epileptic seizures and thus the role of PV in maintaining the stability of neuronal networks was assessed in knockout (PV-/-) mice. Pentylenetetrazole induced generalized tonic-clonic seizures in all genotypes, but the severity of seizures was significantly greater in PV-/- than in PV+/+ animals. Extracellular single unit activity recorded from over 1000 neurons *in vivo* in the temporal cortex revealed an increase of units firing regularly and a decrease of cells firing in bursts. In the hippocampus, PV-deficiency facilitated the $GABA_A$ergic current reversal induced by high-frequency stimulation, a mechanism implied in the generation of epileptic activity. We postulate that PV plays a key-role in the regulation of local inhibitory effects exerted by GABAergic interneurons on pyramidal neurons. Through an increase in inhibition, the absence of PV facilitates synchronous activity in the cortex and facilitates hypersynchrony through the depolarizing action of GABA in the hippocampus.

Introduction

A finely tuned balance between excitatory and inhibitory activity in a neuronal circuit is required for appropriate brain function. Anatomical and/or chemical alterations resulting from changes in excitatory (glutamatergic) or inhibitory (GABAergic) activity can lead to sustained, abnormally synchronous and excessive discharges of large populations of neurons, which is manifested as epileptic seizures (Aird and Gordon, 1993; Bernard *et al.*, 1999; Engel, 1996; Prince, 1999). In the cerebral cortex, γ-aminobutyric acid (GABA)-containing interneurones control pyramidal cell activity, restrict excitation both in a feedback and feedforward manner (Chagnac-Amitai and Connors, 1989; Kisvarday *et al.*, 1994) and are known to be critical to synchronous activity (Jones, 1993; Lytton and Sejnowski, 1991; Somogyi *et al.*, 1998). The subpopulation of inhibitory, GABAergic interneurones expressing the EF-hand calcium-binding proteins parvalbumin (PV) or calbindin-D28k (CB), and in particular PV-expressing chandelier cells play an important role in controlling pyramidal cell excitability (Marco *et al.*, 1996), for review, see (DeFelipe, 1997). These neurons are also thought to be important in the regulation and control of seizure activity (Mihaly *et al.*, 1997). PV is a cytosolic low-molecular weight (M_r 12 kDa), high-affinity Ca^{2+}-binding protein and the intracellular concentration in interneurones was reported to be in the order of 50 μM (Plogmann and Celio, 1993). It has been proposed that efficient Ca^{2+}-buffering by PV and its high concentration in PV-expressing nonpyramidal cells is a prerequisite for the proficient inhibition of cortical networks (DeFelipe, 1997). To investigate this hypothesis, we used mice lacking PV (PV-/-), which had previously been produced by homologous recombination (Schwaller *et al.*, 1999). These mice show no obvious abnormalities when maintained under standard housing conditions and the frequency of homozygous animals is approximately 25% indicating that embryonic development is not altered in these animals. In PV-/- mice, changes in the contraction/relaxation cycle of fast-twitch muscles, which in WT animals contain significant amounts of PV, can be directly correlated with the absence of this slow-onset Ca^{2+}-buffer. The amplitude of a Ca^{2+}-transient after a brief electrical stimulation is not changed, but the initial decay of $[Ca^{2+}]_i$ is significantly reduced in the absence of PV (Schwaller *et al.*, 1999). A similar effect of PV on the kinetics of Ca^{2+}-transients is detected in PV-injected chromaffin cells (Lee *et al.*, 2000b) and more important in a subpopulation of inhibitory hippocampal neurons (Lee *et al.*, 2000a). In terms of the specific function of PV, the kinetics of Ca^{2+}-binding and-release is likely to be of great

importance. We have demonstrated that the lack of PV presynaptically in the axo-axonic (chandelier) and basket cells of the cerebellum affects the paired-pulse modulation at this synapse to the Purkinje cell (Caillard *et al.,* 2000). In WT mice this synapse shows paired-pulse depression which changes to paired-pulse facilitation in PV-/- mice at short time intervals (<100 ms). In the hippocampus, PV-deficiency facilitated repetitive IPSCs at frequencies > 20Hz and the power of related inhibition-based gamma oscillations was increased (Vreugdenhil *et al.*, 2003). Thus, PV is able to affect short-term modulation that likely affects temporal aspects of the entire network containing PV-expressing neurons. In this report, we investigated the effects of PV-deficiency on the stability of cortical neuronal networks. We challenged the networks *in vivo* using the convulsant drug pentylenetetrazole, assessed the firing properties of pyramidal cells in the temporal neocortex *in vivo* and assessed the consequence of facilitation of GABA release with high-frequency activity in hippocampal slices.

Results

Distribution of PV-immunoreactive (PV-ir) neurons and neurons containing similar abundantly expressed Ca^{2+}-binding proteins in the brain of PV-/- mice are not altered

The genotype of each mouse was determined by PCR as described before (Schwaller *et al.*, 1999). The distribution and expression levels of PV were investigated in the three genotypes. Western blot analysis of cytosolic proteins extracted from forebrain or cerebellum revealed the complete absence of a positive signal in PV-/- mice and reduced signal in PV+/- animals compared to the WT ones (**Fig. 1**). A sandwich-ELISA method was used to quantify the amounts of PV present in the different genotypes. In both, the cerebellum and the forebrain the PV content in the heterozygous mice was reduced to 30 - 40% compared to WT mice (Table 1). In this genotype (PV+/-) PV levels in some other organs with significant expression of PV (kidney, fast-twitch muscles *tibialis anterior* and *extensor digitorum longus*) were analyzed and also found to be approximately 30 - 50% compared to WT mice (Table 1). PV-expressing cells are characterized by the presence of "perineuronal nets", a specific extracellular matrix (ECM) containing chondroitin sulphate proteoglycans (e.g. neurocan and phosphacan), which can be visualized by the staining of N-acetylgalactosamine specific lectins (Celio *et al.*, 1998; Kosaka and Heizmann, 1989). Binding sites for

Vicia villosa agglutinin (VVA), *Wisteria floribunda* agglutinin (WFA) or soybean agglutinin (SBA) are present at high densities on the surface of PV-expressing nonpyramidal cells. The developmental expression of PV is in temporal association with the beginning of physiological activity (Solbach and Celio, 1991; Soriano *et al.*, 1992). Thus the question is raised whether the lack of PV in the knockout animals leads to the absence or degeneration of this subpopulation of nonpyramidal cells expressing PV in WT animals. It is also possible that other cell types in the knockout animals replaced the cells originally expressing PV in the WT ones. Our results indicate that the three genotypes (PV+/+, PV+/- and PV-/-) show no apparent alterations in distribution or the number of interneurons throughout the cerebral cortex (**Fig. 2A**) and the multipolar interneurones of the hippocampus ((Vreugdenhil *et al.*, 2003), not shown) in VVA-stained brain sections. A detailed immunofluorescence analysis by laser scanning confocal microscopy on WFA-stained perineuronal nets around cortical interneurones of PV-/- mice revealed no differences compared to WT mice (Haunso *et al.*, 2000). PV-expressing cells not only share a specific staining, they can also be recognized by specific discharge properties. In the rat cortex PV-expressing nonpyramidal cells are characterized as fast-spiking (FS) cells and spike trains elicited by depolarizing current pulses in FS cells show almost no spike-frequency adaptation (Kawaguchi and Kubota, 1993; Kawaguchi and Kubota, 1997). Preliminary results from similar experiments performed on PV-/- mice showed that FS cells with discharge properties identical to WT mice can be identified (M. Galarreta & S. Hestrin, personal communications). Both anatomical and electrophysiological results suggest that the inhibitory interneurones normally expressing PV (including the chandelier and basket cells) were not eliminated or replaced by another subpopulation of nerve cells and are still present in the cortex of PV-deficient mice.

Since in a small population (≈ 5%) of GABAergic interneurones, the Ca^{2+}-binding proteins PV and CB are co-expressed, we investigated whether the number of CB-expressing cells was up-regulated in PV-/- mice. The expression pattern of the closely related protein calretinin (CR) was also analyzed. In all three genotypes the expression patterns of CB- and CR-immunoreactive cells in the neocortex was qualitatively not different (**Fig. 2B**). This was the case for the distribution in the different cortical layers as well as the density of CB- and CR-ir neurons. Western blot analysis of cytosolic proteins isolated from forebrain and cerebellum of PV-/- mice also failed to show any up-regulation of CR or CB (**Fig. 1)** and also no changes

in mRNA levels of CB and CR were observed with micro array analysis (not shown). We cannot discard the possibility that levels of CB in individual neurons expressing both, CB and PV (e.g. Purkinje cells in the cerebellum) are higher than in WT animals to compensate for the lack of PV. In the neocortex and hippocampus, where functional experiments were carried out *in vivo* and *in vitro* (see below), the co-expression of any two of these proteins is a very rare event.

The relative abundance of GABA(R) mRNAs and selected GABA(R) protein is not changed in PV-/- mice

The lack of PV in presynaptic terminals has been show to affect GABAergic transmission as evidenced by altered paired-pulse modulation at the synapse between stellate/basket cells and Purkinje cells (Caillard *et al.*, 2000) and by increased facilitation of repetitive IPSCs in the hippocampus (Vreugdenhil *et al.*, 2003). Thus, we hypothesized that PV deficiency could induce compensation mechanisms such as changes in the amount, distribution or subunit composition of different GABA receptors. At the global level, differential expression analysis between PV+/+ and PV-/- cerebellum and forebrain using cDNA micro arrays containing 96 genes involved in neurotransmission including 13 subtypes of GABA receptors revealed no significant changes except for PV transcripts. At the protein level, semi-quantitative Western blot analysis of the $GABA_A$ receptor subunits $\alpha 2$, $\alpha 3$ and $\beta 2/3$ showed no significant differences between PV-/- and PV+/+ mice (**Fig. 3**).

PV-/- mice manifest a higher sensitivity towards the convulsant drug pentylenetetrazole (PTZ)

Epilepsy, one of the most common neurological disorders, is characterized by massive hypersynchronous discharges from large assemblies of neurons (Traub *et al.*, 1996). Previous findings on altered short-term plasticity and increased power at gamma frequency in PV-/- brain *in vitro* (Caillard *et al.*, 2000; Vreugdenhil *et al.*, 2003) led us to hypothesize that subtle changes in the temporal aspects of network signaling could thus affect the susceptibility to epileptic seizures. We have used pentylenetetrazole (PTZ) to induce acute epileptic seizures (Loscher and Nolting, 1991; Olsen, 1981; Stone and Javid, 1979; Yonekawa *et al.*, 1980

). Animals were injected with PTZ (50 -70 mg/kg i.p.) and the seizure intensity as well as the time until onset of clonic-tonic seizures (CTS) was measured. At the lowest dose tested (50 mg/kg), the average seizure stage was not significantly different in the three genotypes (6.0 ± 0.7, 6.0 ± 0.6 and 6.1 ± 0.2 for PV-/- (n=6), PV +/- (n=6) and PV+/+ (n=12), respectively). At a dose of 60 mg/kg, PTZ **(Fig. 4A)**, the majority of animals (approximately 90%, irrespective of the genotype) showed generalized clonic-tonic seizures, characterized by forelimb and/or hindlimb clonus and tonus resulting in episodes of falling down (seizure stage ≥ 6). While also at 60 mg/kg, PTZ-induced seizures in PV+/+ and PV+/- mice were classified as stage 6, PV-/- mice in the average were classified as stage 7. **Fig. 4B** shows the relative distribution of seizure stages 5 - 8 reached by the three genotypes at 60 mg/kg PTZ. A significant shift towards increased seizure intensity is evident from PV+/+ to PV-/- mice. The percentage of animals reaching *status epilepticus* (SE, seizure stage ≥ 7) was significantly higher in PV-/- mice (78% vs. 16% for WT and PV+/- animals, respectively; **Fig. 4B**). The severity of SE was so intense that 34% of the PV-/- mice and 5% of the PV+/- animals died after the PTZ administration (seizure stage 8), while all PV+/+ animals survived (**Fig. 4B**). At the highest dose tested (70 mg/kg PTZ), a majority of animals went into SE leading to death 66% of PV-/- mice compared to 33% for both, PV+/- and WT animals (**Fig. 4A**). Thus, also at this dose the severity of PTZ-induced epileptic seizures was higher in PV-/- mice compared to the other two groups. As in the electrophysiological recordings, the question of the genetic background was also addressed in the PTZ experiments. For this purpose, a F1 generation between 129/SvEv and C57BL/6J mice were bred and compared with the PV+/+ mice. The susceptibility to 60 mg/kg of PTZ of these mice was not significantly different from the PV+/+ (129P2 x B6) mice (seizure stage: 6.00 ± 0.14 for PV+/+ (n = 18) vs. 6.00 ± 0.19 for F1 129/SvEv x C57BL/6J mice (n = 16).

The onset of seizure activity due to PTZ depends mainly on two parameters: the threshold concentration of PTZ to cause epileptic seizures needs to be reached and a 'critical' mass of neurons needs to be affected. As the concentration of PTZ is increased from 50 to 70 mg/kg, the time of onset of CTS decreased from approximately 300 s to 90 s in all three genotypes **(Fig. 4C)**. This most likely reflects the kinetics of uptake into the vascular system and thus the critical concentration to induce seizures is reached earlier when higher concentrations of PTZ are used. Of note the latency of CTS onset was consistently slightly longer in PV-/- mice at all 3 doses of PTZ tested **(Fig. 4C)**.

The proportions of electrophysiologically-characterized types of cortical neurons are changed in PV-deficient mice

In the light of the reduced seizure threshold we have first assessed the effect of PV deficiency for neuronal networks in the neocortex. Among the interneurons that innervate pyramidal cells of the cortex, are PV-immunoreactive (PV-ir) chandelier and basket cells which are proposed to play an important role in the control of pyramidal cell excitability (Blümcke *et al.*, 1990; Cauli *et al.*, 1997; DeFelipe *et al.*, 1993; DeFelipe *et al.*, 1989; Hendrickson *et al.*, 1991; Hendry *et al.*, 1989; Lewis and Lund, 1990). Thus, it is expected that any alteration in the functional properties of the PV-ir interneurones will modify local inhibition, which eventually may affect the collective activity of the whole neuronal network. Extracellular single unit recordings from the temporal cortex were performed in Equithesin-anesthetized mice by means of four independently advanced microelectrodes. We analyzed the three genotypes (PV+/+, PV+/-, PV-/-, n = 6 subjects for each genotype group). Since the PV-/- strain has a mixed 129P2 x B6 background and were maintained as homozygous strains (PV+/+ and PV-/-) for several generations, a genetic drift between the two genotypes could not be excluded *a priori*. Thus, we included in each genotype group half of subjects with a 129SvJ background (as defined in Materials and Methods). The recordings were performed along the same angle of electrode penetrations (40° off the vertical line) for all subjects. The median depths were 835µm, 755µm, 800µm and the interquartile ranges 825µm, 855µm and 825µm in PV+/+, PV+/-, and PV-/- mice, respectively. No significant difference between the three groups could be observed with respect to the electrode depth of the recording sites. The electrode tips were mainly positioned in layers III-IV and the deepest recording of a series was largely confined to layer V according to a stereotaxic atlas of the mouse brain. A total amount of 1161 single units were recorded during spontaneous activity. The signals of 39 units changed during the experimental session and were discarded from the analysis. Recordings from an overall number of 1122 single units were analyzed (354, 397, and 371 in PV+/+, PV+/-, and PV-/- mice, respectively). The time series of the spikes -the spike trains- were analyzed by the autocorrelation technique (Abeles, 1982) and three cell types were defined by the temporal course of their discharge pattern. The 'regular' cells were characterized by a flat autocorrelogram with a trough near time zero, thus indicating a tendency to discharge following a Poisson distribution (**Fig. 5A**). The refractoriness (i.e. the

duration of the trough near time zero measured on the autocorrelogram) of the regular spiking units was approximately 14 ms. The remaining single units showed a tendency to fire isolated spikes intermingled with bursts, as indicated by a hump in the autocorrelogram near time zero. According to the average burst duration and intraburst frequency it was possible to distinguish two classes of units. The first type was termed 'irregular' (**Fig. 5B**) and the second type, termed 'bursting' (**Fig. 5C**), was characterized by longer burst duration and low rate bursting, at frequencies less than 30 Hz. The average burst size was estimated by the area of the hump in the autocorrelogram (Abeles, 1982; Villa, 1990) and was about 1.7 spikes for both irregular and bursting units (the burst size is always equal to 1 in 'regular' firing units). For all groups of animals the firing rate of both regular and bursting firing cells was statistically similar, but it was higher than the rate of discharges of irregular units (t-test, $P < 0.01$).

The characteristics of the discharge pattern of all type of units were consistently the same in the three genotypes (Table 2). Conversely, the distribution of the unit types within the experimental animals was significantly different (contingency table analysis, Chi-square = 63.1, $P < 0.001$) as illustrated in **Fig. 5D**. The main finding is that in PV-/- subjects the proportion of single units characterized by a regular Poisson pattern of discharges tended to be increased. On the opposite, the percentage of single units classified as bursting type was smaller in PV-/- mice. In PV+/- mice with neuronal PV levels, which are approximately one third of the ones found in PV+/+ animals (Table I), a shift from bursting firing to irregular firing was observed. It is also interesting to note that in PV-deficient mice the spontaneous firing rate (1.37 ± 0.08 spikes/s, average ± S. E. M.) of all types of cells pooled together was significantly higher than in WT (1.12 ± 0.06 spikes/s) and heterozygous animals (1.10 ± 0.05 spikes/s). The comparison between PV-/- and PV+/+ in mice with a 129SvJ genetic background revealed similar results to the ones obtained in the mixed background. This suggests that the observed change from “bursting” firing to “regular” firing pyramidal neurons is likely to be the result of the deletion of the functional PV gene and not due to differences in the genetic background of PV+/+ and PV-/- mice with the mixed B6x129P2 genetic background. The influence of the genetic background in different knockout strains has been discussed in great detail (Gerlai, 1996; Zimmer, 1996) and is principally concerned with behavioral differences of different strains. Nonetheless, also electrophysiological recordings *in vivo* might be susceptible to variations of the genetic background,

but the similar results we have obtained with the two PV-/- lines is in support of an effect due deletion of the functional PV gene.

PV deficiency promotes depolarizing IPSCs in hippocampus

We next assessed the effect of PV deficiency on neuronal networks in the epilepsy-prone hippocampus. Hippocampal PV interneurons are organized in a network of interconnected cells and are thought to significantly affect network properties (Bartos *et al.*, 2002; Fukuda and Kosaka, 2000). It has been previously demonstrated that PV-deficiency facilitated repetitive IPSCs and related inhibition-based gamma oscillations in the hippocampus (Vreugdenhil *et al.*, 2003). Here, we recorded monosynaptic $GABA_A$ergic IPSCs in hippocampal slices evoked by stimulation of the near stratum pyramidale. Under our experimental conditions, the postsynaptic responses were completely blocked by 50 µM bicuculline methiodide and therefore mediated by $GABA_A$ receptors (data not shown). At maximal IPSP stimulus intensity the $GABA_A$ergic IPSC had shown a late current reversal (Vreugdenhil *et al.*, 2003). At this intensity a train of 20 pulses at 100 Hz induced a hyperpolarisation followed by a massive slow depolarization in cells recorded in current clamp mode (**Fig. 6A**). The addition of the $GABA_A$ receptor antagonist bicuculline methiodide (50 µM) completely blocked the slow depolarization (Herrero *et al.*, 2002) and unmasked a depolarization associated with the stimulus train (4 out of 4 cells from 3 control mice tested), which in turn was blocked by the metabotropic glutamate receptor group I antagonist (S)-3-carboxy-4-hydroxyphenylglycine (50 µM; **Fig. 6A**). The maximum depolarization was 14.2 ± 2.6 mV for 7 cells from 6 PV-/- mice and 9.3 ± 2.4 mV for 9 cells from 7 PV+/+ mice (n. s.). The slow depolarization evoked action potential trains in 5 out of 7 (71%) cells from PV-/- *versus* 3 out of 9 (33%) cells from PV+/+. In voltage-clamp mode the cells responded with a sustained inward current following an initial outward current, which was blocked by bicuculline (**Fig. 6B**), indicating that current reversal is mainly due to bicarbonate efflux after collapse of the chloride gradient (Davies and Collingridge, 1993; Kaila, 1994). We have not further explored the contribution of a GABA activity-dependent potassium transient to the late phase of the depolarization (Bracci *et al.*, 1999; Kaila *et al.*, 1997). The contribution of the small remaining metabotropic glutamate receptor group I-sensitive inward current (Congar *et al.*, 1997) was restricted to the duration of the tetanic stimulus (**Fig. 6B**). Despite the relatively small first outward IPSC (-0.6 ± 0.2 nA

versus –0.9 ± 0.3) the peak amplitude of the slow inward current in PV-/- cells did not differ significantly from that for PV+/+ cells (0.8 ± 0.1 nA. *versus* 0.5 ± 0.1 nA; $P < 0.09$). But more importantly, the reversal of the IPSC occurred significantly earlier in cells from PV-/- mice (255 ± 34 ms after the onset of the stimulus train *versus* 377 ± 51 ms, Student-*t*-test $P < 0.05$). Thus, PV-deficiency accelerates the $GABA_A$ergic current reversal induced by high-intensity high-frequency stimulation.

Discussion

Expression of other CaBPs, neurotransmitter receptors and morphology of "PV-neurons" in PV-/- mice

In recent years, a wealth of work has been published on the distribution of particular calcium-binding proteins including PV, CB and calretinin (CR) (for a review, see (Andressen *et al.*, 1993; Baimbridge *et al.*, 1992; DeFelipe, 1997), but much less is known about the functional significance of these proteins. Although their affinities for Ca^{2+} are all in the submicromolar range, they are expressed in distinct, mainly non-overlapping populations of neurons suggestive of specific functions. Ideas about these "specific" functions remain relatively vague and include such general functions as involvement in Ca^{2+}-buffering, Ca^{2+} homeostasis and also are role in the protection against excitotoxicity has been proposed, but results on the latter aspect are controversial (e.g. Hartley *et al.*, 1996; Klapstein *et al.*, 1998; Meier *et al.*, 1997)). Within the last years, knockout mice for the three proteins PV (Schwaller *et al.*, 1999), CB (Airaksinen *et al.*, 1997) and CR (Schiffmann *et al.*, 1999) have become available and have been used to address some of these questions (Schwaller *et al.*, 2002). Interestingly, the expression patterns of the other two proteins in either CB-/- (PV, CR) or CR-/- (PV, CB) mice were not significantly changed and also global expression levels determined by Western blot analysis were not altered. These results are in good agreement with our findings that neither the distribution nor the levels of CR and CB were affected by the lack of PV. This suggests that at least at the level of these three proteins no compensatory mechanism is induced by the lack of either one of these. Furthermore, the lectin-staining of the "perineuronal" nets -a characteristic accumulation of extracellular matrix molecules in intimate contact with the surface of PV-expressing neurons (Celio and Blümcke, 1994)- with either VVA (this report) or *Wisteria floribunda agglutinin* (WFA) (Haunso *et al.*, 2000) revealed the "PV neurons" to be present in the neocortex. Neither analysis at the global level (this report), in the hippocampus (Vreugdenhil *et al.*, 2003) nor in refined detail by fluorescence microscopy (Haunso *et al.*, 2000) revealed any differences of the perineuronal nets in PV-/- mice suggesting morphologic and metabolic entireness of these neurons. These findings were additionally supported by the identification of fast-spiking (FS) cells in the PV-deficient mice, which also indicates an intact functional activity. In summary, all the available information suggest that the lack of the slow-onset Ca^{2+}-buffer PV does not substantially affect the distribution, morphology and basic electrophysiological properties of the subpopulation of cortical interneurons normally expressing PV. These findings are in

excellent agreement with previous ones on the cytoarchitecture of the hippocampal formation in PV-/- mice, where no differences in the number, distribution, or morphology of interneurons compared to wild-type mice were observed (Bouilleret *et al.*, 2000). Quantitative analysis of the number of VVA-positive cells per length of pyramidal layer revealed these not to be different between PV+/+ and PV-/- mice (Vreugdenhil *et al.*, 2003). Additionally, immunohistochemistry for the $GABA_A$ receptor subunits $\alpha 1$, $\alpha 2$ and $\beta 2/3$ showed no apparent differences when comparing neocortical regions of PV-/- and PV+/+ mice (J.-M. Fritschy, personal communication). This is line with our results from semi-quantitative Western blots using different antibodies against $GABA_A$ receptor subunits. Analysis of $GABA_A$ receptor subunit mRNA levels by DNA chip technology also revealed no significant differences between genotypes in cerebellum and forebrain. In these experiments no changes in abundance of other neurotransmitter receptor mRNAs including different types of glutamate receptors or peptide receptors were observed (data not shown). Although subtle changes at the level of $GABA_A$ receptors cannot be entirely excluded, we currently do not have any indications for such changes in PV-deficient mice. In addition we cannot rule out the possibility that differential expression could take place only in a subpopulation of cells and would not be detected in complex tissues such as forebrain or cerebellum.

PV-deficiency and susceptibility to epileptic seizures

PTZ-induced seizure onset is known to be localized in deep brain structures spreading to the hippocampus and neocortex (Binnie *et al* 1985). Thus, hippocampus and neocortex are involved in seizure spread and its behavioral expression rather than in seizure initiation. Although there were no differences at low doses of PTZ and the time interval until onset of clonic-tonic seizures was longer in PV-deficient mice, the seizures were more severe. This suggests that these mice display facilitated seizure spread in cortical areas despite an increased threshold to seizures in these areas. Previously we did not notice a change in the expression of kainate-induced seizures in PV-/- mice (Bouilleret *et al.*, 2000), but since a detailed morphological analysis was the principal aim of this study no electroencephalogram analysis was carried out. The relation between PV and epilepsy has been established in various studies. Evidence was provided that PV is lost from GABAergic perikarya of adult gerbils with repeated clonic/tonic seizures, while gerbils showing no seizure activity retain a high number of PV neurons in the CA1 region of the hippocampus (Scotti *et al.*, 1997).

Multiple small regions with abnormal patterns of immunostaining for PV and glutamic acid decarboxylase (GAD) have been observed in human neocortex resected during surgical treatment of intractable temporal lobe epilepsy (Marco *et al.,* 1996). In these patients the PV immunoreactivity of GAD-ir neurons was reduced, a finding that is compatible with at least two interpretations: i) the disappearance of neurons normally expressing PV or ii) down-regulation of PV in this cell population. If the latter one is assumed and since PV-ir GABAergic neurons include chandelier cells and basket cells that exert powerful regulation of impulse generation in cortical pyramidal cells (DeFelipe, 1999), this might implicate that in the absence of PV crucial perisomal inhibition is increased in these networks. In the hippocampus of rats subjected to two experimental models of temporal lobe epilepsy (TLE), Cossart *et al.* (2001) reported that dendritic GABAergic inhibition was reduced likely due to the loss of a subgroup of interneurons (O-LM cells), which project on the distal dendritic tree of principal cells. On the other hand, perisomatic projecting interneurons (presumably PV-ir basket cells) remained intact and were found to be hyperactive in that model of TLE. The authors proposed that the increased somatic inhibition could provide a means to keep the network under the control most of the time. Interestingly, this idea has been challenged in several reports, where an increased rather than a decreased inhibition was detected (Otis *et al.,* 1994; Prince and Jacobs, 1998). Theoretical analysis suggests that an increase of inhibition in networks of interneurons contributes to synchronization of their firing and that of principal cells (Di Garbo *et al.,* 2002). In a mathematical model of layer V cortical neurons, Bush *et al.* (1999) "induced" epileptiform activity by increasing pyramidal cell excitability, which was often paralleled by increased perisomatic inhibition. Increased inhibition was actually observed experimentally in postlesional epileptogenic slices (Prince *et al.*, 1997) supporting the "counter-intuitive" hypothesis of increased inhibition facilitating ictogenesis. This is in line with previous findings that GABA or GABA-enhancing substances can induce epileptiform activity (Kaila *et al.*, 1997; Lopantsev and Avoli, 1998). Also in other epilepsy models, GABA-mediated inhibition is increased (Traub *et al.*, 1996). Interestingly increasing GABA release with a $GABA_B$ receptor antagonist, which increases GABAergic depolarizations (Bracci *et al.,* 1999) aggravates PTZ-induced seizures (Veliskova *et al.,* 1996). The slightly delayed onset of the clonic-tonic seizures is also in line with a stronger inhibition. While in cortical areas a slight reduction of inhibition can cause epileptiform activity

(Whittington *et al.*, 1995), a stronger inhibition may delay the point where PTZ disables inhibition beyond that critical level.

Lack of PV and firing pattern of cortical pyramidal neurons

Our PTZ results show that the absence of PV is correlated with a modification of the inhibitory functions normally exerted by nonpyramidal cells of the temporal neocortex. An *in vitro* analysis of layer V cortical cells in the rat revealed different electrophysiologically-defined classes including regular spiking cells (RS_1 and RS_2) and intrinsically bursting cells (IB) based on action potential firing in response to current injection (Hefti and Smith, 2000). A strict definition of RS_1, RS_2 and IB cells was not always possible and the authors proposed the existence of a kind of continuum of firing properties with RS_1 an IB cells being the extreme on the scale. In our *in vivo* electrophysiology experiments, we defined three categories of cells based on their spontaneous firing pattern as regular, irregular or bursting cells with a likely correlation to RS_1, RS_2 and IB cells, respectively. While in the complete absence of PV in PV-/- mice, a shift in the proportion of cells with bursting firing characteristics to regular firing ones was observed, the reduced amount of PV in the PV+/- neurons had an intermediate effect indicative of a gene-dosage effect. This is reflected by the increased proportion of irregular firing cells, while the decrease in the proportion of bursting firing cells was much less pronounced than in PV-/- animals.

How can we reconcile the differences in firing properties of pyramidal cells and the increased control of inhibition in PV-/- mice? I) According to Hefti *et al*. (Hefti and Smith, 2000) IB cells are characterized by their greater ability to fire short bursts of action potentials in response to thalamocortical stimulation and the amount of inhibitory input is much smaller than in RS cells. Thus, an increase in the ratio of RS vs. IB cells could be interpreted as an increase in inhibition. II) Pharmacological experiments using the $GABA_A$ receptor agonist muscimol and the benzodiazepine receptor agonist flurazepam in combination with electrophysiological recordings from the somatosensory cortex of anesthetized rats (Oka *et al.*, 1993) revealed two distinct firing patterns (regular spiking and bursting). Inhibition of cells characterized by bursting pattern of firing was significantly weaker than in cells displaying the regular spiking pattern. III) Our previous experiments on short-term plasticity with PV-/- mice, i.e. facilitated paired-pulse modulation between PV-ir basket and Purkinje cells in the cerebellum (Caillard *et al.*, 2000) and facilitated repetitive

IPSCs at frequencies > 20 Hz in the hippocampus (Vreugdenhil *et al.*, 2003), are all in support of increased inhibition in the absence of PV. The highest density of PV-ir neurons and innervation in the rodent neocortex is located in layers III-V (for a review, see Hof *et al.,* 1999), the region where most of the *in vivo* extracellular activity presented here was recorded. Thus, the decreased ratio of bursting cells in PV-/- subjects observed in our extracellular electrophysiological recordings is in agreement with the above-mentioned studies and may well be associated with increased local inhibitory effects due to the lack of PV in GABAergic cells. It can not be excluded that other secondary not yet identified effects resulting from the inactivation of the PV gene may also contribute to the observed changes in the proportions of pyramidal cells with distinct firing patterns.

Increased inhibition and network effects

Although intuitively facilitated GABA release is not expected to be epileptogenic, when GABAergic inhibition is challenged it can turn into a depolarizing driving force, involved in seizure initiation (Kohling *et al.*, 2000); Fujiwara-Tsukamoto *et al.*, 2003). In the present study we observed that in hippocampal slices the $GABA_A$ergic current reversal induced by high-frequency stimulation of the IPSC occurred significantly earlier in cells from PV-/- mice compared to wild-type controls. These so-called GABA-mediated depolarizing postsynaptic potentials (Kaila *et al.*, 1997) previously reported in CA1 pyramidal cells evoked by high-frequency stimulation are characterized by their large amplitude and prolonged duration. In the rat entorhinal cortex, 4-AP-induced NMDA-dependent synchronous activity leading to ictal-like epileptiform discharges have been demonstrated to be mediated via a $GABA_A$-ergic mechanism (Lopantsev and Avoli, 1998). Furthermore, depolarizing GABA responses were observed in slices of human cortical tissue from epilepsy surgery (Deisz *et al.*, 2002) and were also shown to contribute to intericatal activity in human temporal lobe epilepsy (Cohen *et al.*, 2002). Here we report that PV-deficiency facilitates the pro-convulsive GABA-mediated depolarizing postsynaptic potential in the hippocampus. Due to the similarity of the hippocampal and neocortical network of PV-ir neurons with respect to GABAergic projections to pyramidal neurons exerted by these neurons –and also based on previous ultrastructural, immunohistochemical and functional data– we propose that this facilitation may occur in the neocortex as well, although this remains to be proven. In support of this hypothesis are the findings that short-term

modulation was facilitated in the absence of PV, both in the cerebellum (Caillard *et al.*, 2000) and hippocampus (Vreugdenhil *et al.*, 2003) indicating that PV has a similar function in the different interneuron populations.

Model of the role of PV in neuronal networks

Based on the assumption that PV-deficiency is likewise manifested in both, *in vitro* and *in vivo* recordings of hippocampal and neocortical pyramidal neurons, respectively and data from previous *in vitro* studies on the Ca^{2+}-buffering properties and the deduced function of PV have led us to propose the following model. Delayed Ca^{2+}-buffering by PV helps to increase the initial decay of $[Ca^{2+}]_i$ in presynaptic PV-containing terminals. In its absence, residual $[Ca^{2+}]_i$ remains elevated for longer periods, which favors short-term facilitation at relatively short (< 50 ms) inter-spike intervals. In PV-/- mice, increased facilitation is translated into increased inhibition in networks consisting of normally PV-containing interneurons and pyramidal cells. This, in turn shifts the firing properties of a fraction of pyramidal cells from “bursting” to a “regular” firing pattern. Such “regular” discharge pattern in the cerebral cortex is associated to a coincidence-detector mode of functioning of pyramidal cells (Abeles, 1991). In this mode the pyramidal cell is able to generate an action potential because the gain of several synchronous EPSPs is much larger than the sum of their asynchronous inputs. That is, less input, which is synchronized in time, is more effective and tends to be transmitted through the cerebral network with synchronous volleys (Diesmann *et al.*, 1999). Preliminary analyses of local field potentials in PV-deficient mice indicate a tendency to an increased area of synchronization (Villa *et al.*, 2000). We propose that the shift in the firing pattern observed in the PV-/- mice increases the probability of activating synchronous firing over a larger area and thus to an increased susceptibility towards epileptogenic insults such as the ones induced by PTZ.

In conclusion, we suggest that the absence of PV in the subpopulation of GABAergic interneurones modifies the dynamics of the inhibitory control at the local level. Although the extent of this modification may vary in brain region-specific PV-ir populations, we may postulate the following generalized hypothesis: During normal spontaneous activity this change in the dynamics of the inhibitory control leads to an increase in inhibition. However when networks are further challenged by inputs that affect cellular

excitability the facilitated inhibition may turn into a depolarizing force, allowing hypersynchronous neuronal activity to propagate over larger networks, thus facilitating seizure initiation and/or spreading.

Experimental Procedures

Generation of PV-deficient mice and breeding

Mice with two different genetic backgrounds were used in this study. The first group of mice are a mixed background of 129/OlaHsd x C57BL/6J (129P2xB6) and are named PV-/-. In the second group the chimeric mice derived from injection of targeted embryonic stem cells (E14/Ola (Hooper *et al.*, 1987)) in the blastocysts of C57BL/6J mice were mated to 129/SvEv mice resulting in the 129PV-/- line (129/OlaHsd x 129/SvEv). Electrophysiological experiments were carried out with both groups of mice. In the PTZ studies, besides the WT animals with a mixed 129/OlaHsd x C57BL/6J background, a F1 generation between 129/SvEv and C57BL/6J mice were bred and were not found to be significantly different from the PV+/+ mice in this assay. Biochemical analysis (Western blot, ELISA) and immunohistochemistry was performed with the 129/OlaHsd x C57BL/6J (PV-/-) mice.

PCR analysis for genotyping

From all mice used in the experiments a small tail biopsy (2-3 mm in length) was taken and genomic DNA was isolated using a commercial kit (Invitrogen, Groningen, The Netherlands) and 300 ng of purified DNA were used per PCR reaction. For the genotyping of the animals 2 PCR reactions were carried out. The strategy makes use of the fact that in the mutated allele, the majority of the coding sequence has been replaced by a neo-cassette (Schwaller *et al.*, 1999). Amplification of exon 3 gives rise to a fragment of 151 bp, while amplification of a part of the neo-resistance leads to one of 188 bp. The former confirms the presence of a wild-type allele and the latter a mutated one. The PCR protocol used is the following: 94°C for 2 min, 72°C for 10 s (addition of Taq Polymerase (DyNAzyme II, Bioconcept, Allschwil, Switzerland) at this point) followed by 40 cycles (94°C for 20 s, 68°C for 40 s and 72°C for 40 s).

Immunohistochemistry

Immunohistochemical analysis of floating cryostat brain sections (40 µm thickness) was performed as described by Celio et al. (Celio and Heizmann, 1982), with the exception that the bound primary antibody was revealed by the avidin-biotin technique instead of the peroxidase-anti-peroxidase one. For the

immunostaining the following antibodies were used: anti-parvalbumin PV4064 (1: 5000; Swant, Bellinzona, Switzerland), anti-calbindin D-28k CB300 (1:5000; Swant) and anti-calretinin CR7696 (Schwaller *et al.*, 1993). The perineuronal nets around parvalbumin-expressing neurons were visualized with peroxidase-labeled isolectin B4 *Vicia Villosa* agglutinin (VVA, Sigma L-5641, Buchs, Switzerland) as described (Lüth *et al.*, 1992).

Western blot detection of PV in the forebrain and cerebellum

The brains were removed from sacrificed mice and separated into forebrain and cerebellum, and Western blots performed with the same antibodies against PV, CB and CR as above as previously described (Schwaller *et al.*, 1993).

Semi-quantitative Western blot analysis of $GABA_A$ receptor subtypes

Forebrain samples were homogenized and 60µg (α2, α3) or 20µg (β2/3) of total protein extract were separated by SDS-PAGE (10% PAA gels). Proteins were transferred to blotting membranes and probed with antibodies against α2, α3 and β2/3 $GABA_A$ receptor subunits as described before (Mohler *et al.*, 1995) (kind gift from J. - M. Fritschy, University of Zurich, Switzerland)

ELISA

Quantitative results on PV content in the forebrain and cerebellum of WT, PV+/- and PV-/- mice were obtained by a sandwich-ELISA method. The procedure for PV (Caillard *et al.*, 2000) is essentially the same as for the detection of CR as described in detail previously (Schierle *et al.*, 1997). Briefly, for the coating of the ELISA plates, the monoclonal antibody PV235 is used and the bound PV is detected by the polyclonal rabbit antiserum PV4064. All samples were measured in triplicates and samples were taken from 2 animals of each genotype.

Electrophysiological recordings *in vivo*

The genotype of all tested animals was revealed to the experimenter only after measurements were done and calculations had been performed. The animals (6 of either genotype, 32.8 g body weight on average)

were anesthetized with an i.p. injection of Equithesin (0.035 ml/g body weight) at a dose corresponding to 130 mg/kg chloral hydrate and 30 mg/kg of pentobarbital. Equithesin was prepared from a solution of chloral hydrate and pentobarbital sodium (Li and Kelly, 1992) and was shown to preserve subtle response patterns in the auditory midbrain (Li and Kelly, 1992). The animals were mounted in a stereotaxic apparatus without ear bars. The limb withdrawal reflex was checked regularly in order to monitor the depth of anesthesia. Body temperature was monitored permanently and maintained between 37 and 39°C, by means of a heating pad. Four to five independently driven tungsten-glass insulated microelectrodes were advanced stepwise in the temporal cortex (Villa *et al.*, 1999). We aimed to be nearly perpendicular to the surface of the temporal cortex and the angle of penetration of the electrodes was set to 40 degrees with respect to the vertical line. Generally, six sets of recordings were performed in one mouse, the first one in layer II, a majority (four) in layers III and IV and the last one in layer V. Whenever electric signals corresponding to good extracellular spikes were observed the procedure to sort single units from one electrode signal was started by means of a commercial device (MultiSpike Detector, Alpha Omega Engineering) based upon digital signal processing and an on-line template matching algorithm to detect and sort spike waveforms. Up to three different extracellular waveforms (reflecting discharges of three distinct neurons) were discriminated from each microelectrode, with a maximum number of 15 cells being recorded per cell group. The electric impedance of our microelectrodes was about 1-2 MΩ, an unfavorable value to record the extracellular electric fields generated by small neurons. On the basis of our experience we assume that the population of extracellular recorded units corresponded mainly to pyramidal cells and no systematic bias in recording particular cell types in the different genotypes are expected. After isolation of 10 - 15 single units, a recording session lasting approximately 1 hour was started. The spike firing times of each unit were given by interrupts generated by a digital acquisition board (National Instruments NB-32F) driven by an external clock with an accuracy of 1 ms and stored digitally for off-line analyses. Time domain analyses including autocorrelation histograms (Perkel *et al.*, 1967a; Perkel *et al.*, 1967b) were calculated from the time series formed by the spike firing times (i.e., the spike trains) using established methods (Abeles, 1982).

Electrophysiology *in vitro*

Adult mice, randomly selected from both groups (PV+/+ and PV-/-) and from controls, were anaesthetized by intraperitoneal injection of a ketamine (75 $mg.kg^{-1}$) / medetomidine (1 $mg.kg^{-1}$) mixture and then killed by cervical dislocation. The brain was quickly removed from the skull and chilled in ice-cold artificial cerebrospinal fluid (aCSF). The composition of the aCSF was (in mM): NaCl, 125; KCl, 3; $NaHCO_3$, 26; NaH_2PO_4, 1.25; $CaCl_2$, 2; $MgCl_2$, 1; *D*-glucose, 10; pH was equilibrated at 7.4 with a 95% O_2/5% CO_2 gaseous mixture. For the recording of $GABA_A$ergic responses the brain was cut into 400 µm thick transverse slices, using a Vibroslice (Campden Instruments Ltd. Sileby, UK.). Slices were transferred to a recording chamber (sustained at 33 °C), wherein they were maintained at the interface between a warm moist gaseous atmosphere (95% O_2/5% CO_2) and aCSF, flowing at a rate of 2 ml/min. The aCSF was supplemented with 20 µM 6-Nitro-7-sulphamoylbenz[f]quinoxaline-2,3-dione (NBQX), 25 µM *D*-2-amino-5-phosphonovaleric acid (APV), 1 µM CGP 55845A, 5 µM atropine sulphate and 5 µM naloxone hydrochloride, in order to isolate $GABA_A$ergic responses and minimize presynaptic suppression by $GABA_B$ receptors (Davies and Collingridge, 1993; Lambert and Wilson, 1994), muscarinic receptors (Hajos *et al.*, 1998) and µ opioid receptors (Lambert *et al.*, 1991), respectively. In order to promote facilitation (Lambert and Wilson, 1994; Thomson, 1997), the release probability was reduced by increasing the concentration of $MgCl_2$ to 3 mM. Brain slices were allowed to equilibrate for 1 hour before the onset of recording. Monosynaptic $GABA_A$ergic responses were evoked by electrical stimulation (0.1 ms square pulse) using a constant voltage stimulus isolator (Digitimer, Welwyn Garden City, England). The stimulus was applied with a bipolar electrode, constructed from a pair of insulated and intertwined 50 µm diameter nickel/chromium wires (Advent Research Materials Ltd., Halesworth, UK), placed in the pyramidal cell layer of area CA1b, within 0.1 mm from the recording site. Intracellular current-clamp and single-electrode voltage-clamp recordings were taken from neurons within the stratum pyramidale using sharp pipettes filled with 2 M potassium methylsulphate (tip resistance was 50-70 MΩ) connected to an Axoclamp-2A amplifier (Axon Instruments, Burlingham, CA, USA). Impaled cells were first inspected in current-clamp and accepted for recording when the resting membrane potential was at least –55 mV and when the current injection-induced overshooting action potentials. For current-clamp recordings, the resting membrane potential was manually adjusted to –65 mV. Single-electrode switch voltage-clamp recordings were

accepted when the switching rate was > 4 kHz and voltage clamp efficiency was > 90 %, as judged from the difference in the inhibitory postsynaptic potential (IPSP) amplitude between voltage-clamp and current-clamp recordings. The holding potential was –65 mV. Single and double-pulse stimulations were applied at 15-s intervals and stimulus trains (ten pulses) were applied at 3-min intervals.

NBQX, APV, naloxone hydrochloride, atropine sulphate and (S)-3-carboxy-4-hydroxyphenylglycine (CPG) were obtained from Tocris-Neuramin (Bristol, UK), Signals were band-pass filtered (1 Hz – 3 kHz) and sampled at a rate of 10 kHz using a CED 1401 interface and Signal software (Cambridge Electronical Design Ltd., Cambridge, UK). Current traces were digitally filtered off-line. The power of the oscillations was measured by performing fast Fourier transformations over five consecutive 10 s traces. Cross-correlation analysis between field potentials was made over five consecutive traces, using Spike2 software (Cambridge Electronic Design Ltd., Cambridge, UK).

PTZ experiments

Experiments were carried out according to the NIH guidelines for the Care and Use of Laboratory Animals, the European Committee Council Direction of November 24, 1986 (86/69/EEC) and in accordance with the Veterinary Office of the Canton of Fribourg, Switzerland. The number of animals used in the PTZ experiments was kept to an absolute minimum. A total of 117 male and female adult mice were used in this study; 36 PV+/+, 31 PV+/-, 34 PV-/- mice and 16 F1 129/SvEv x C57BL/6J WT animals. Seizures were induced by convulsant doses of PTZ (Sigma, Buchs, Switzerland; 50 - 70 mg/kg i.p.) and numbers of animals (PV+/+, PV+/-, PV-/-) that were tested with different doses of PTZ are the following: at 50 mg PTZ (12, 6, 5), at 60 mg (18, 19, 23) and at 70 mg (6, 6, 6), respectively. The genotype of mice for testing seizure susceptibility was masked until the end of experiments. The seizure intensity was recorded using the following scale: 1) decreased locomotor activity; 2) twitching either of the whole body or localized; 3) one to 20 myoclonic body jerks during the 10-min period; 4) more than 20 myoclonic body jerks during the 10-min period; 5) clonic forelimb convulsions; 6) generalized tonic-clonic seizures, characterized by forelimb and/or hindlimb clonus and tonus resulting in episodes of falling down; 7) status epilepticus (SE); 8) death. Similar scaling of PTZ-induced seizure intensities in mice has been reported before (Ferraro *et al.*,

1999). Animals were observed during a 20-min period. The latency of onset of clonic-tonic seizures was recorded as well as the mortality rate.

Statistics

The firing parameters (sample sizes consisting of the extracellular recorded units varied between n = 76 and n = 199) followed Gaussian distributions (Kolmogorov-Smirnov test) and were analyzed by Student t-test. The distribution of unit types (bursting, regular, irregular) within experimental groups was evaluated by contingency table analysis (Chi-square test) and the significance level was set at $P < 0.01$. In the PTZ experiments, differences between the three genotypes at 60 mg/kg PTZ were corroborated by a non-parametric Kruskal-Wallis test and P-values < 0.05 were considered significant. For comparison between two genotypes, the Mann-Whitney U-Test was used and differences were considered significant at $P < 0.05$.

cDNA micro array analysis:

Microarray analysis was performed from mRNA extracted from 3 to 6 months-old male mice using the one-step method Fastrack (Invitrogen). In order to reduce inter-individual variability, each genotype was constituted by pools of tissues from 5 different mice. DNA microarray technology was performed on microscope polylysine coated slides using the technology developed by Patrick Brown at Stanford (Eisen and Brown, 1999; Schena *et al.*, 1995) and adapted at ESPCI (Potier *et al.*, 2002). The list of genes present on the array can be found at http://www.bio.espci.fr/~puces/neuropuces.html. Briefly, PCR products were spotted on polylysine-coated slides using the Omnigrid from Genemachine (California) with MicroQuill 1000 (Majer Precision, Inc.). Microarrays were hybridized with fluorescent targets obtained by reverse transcription of mRNA from PV-/- and PV+/+ littermates cerebella and forebrains at 60°C in 3.4 X SSC, 0.28% SDS overnight. After washing, the slides were scanned on the General Scanning (Scanarray 3000) capable of analyzing Cy3 and Cy5 fluorescence on spots at a resolution of 10 µm per pixel. Scanned images were then analyzed with the image analysis software Imagene 4.1 (Biodiscovery Inc.). Data were normalized using either a lowess fit or a linear regression on a set of control genes. Statistical analysis was

performed using VARAN and the error model generated from control experiments (NT lowess 0.99, p=0.01 in Varan Analyzer; http://www.bionet.espci.fr/varan/varan_info.html; Golfier et al, in preparation).

Acknowledgments

We would like to thank S. Eichenberger for taking care of the animal facilities and B. Belser for excellent technical support in histochemical methods. The project was supported by the Swiss National Science Foundation (grant: 3200-059559.99/1 to M. R. C. and grants: 3100-063448.00/1 and 3100A0-100400/1 to B. S.) and Novartis.

References

Abeles, M., (1982). Quantification, smoothing, and confidence limits for single-units' histograms. J Neurosci Methods 5, 317-25.

Abeles, M., 1991. Corticonics: Neural Circuits of the Cerebral Cortex. Cambridge University Press, Cambridge, pp. 280.

Airaksinen, M. S., Eilers, J., Garaschuk, O., Thoenen, H., Konnerth, A. and Meyer, M., (1997). Ataxia and altered dendritic calcium signaling in mice carrying a targeted null mutation of the calbindin D28k gene. Proc Natl Acad Sci U S A 94, 1488-1493.

Aird, R. B. and Gordon, N. S., (1993). Some excitatory and inhibitory factors involved in the epileptic state. Brain Dev 15, 299-304.

Andressen, C., Blümcke, I. and Celio, M. R., (1993). Calcium-binding proteins: selective markers of nerve cells. Cell Tissue Res. 271, 181-208.

Baimbridge, K. G., Celio, M. R. and Rogers, J. H., (1992). Calcium-binding proteins in the nervous system. Trends Neurosci. 15, 303-308.

Bartos, M., Vida, I., Frotscher, M., Meyer, A., Monyer, H., Geiger, J. R. and Jonas, P., (2002). Fast synaptic inhibition promotes synchronized gamma oscillations in hippocampal interneuron networks. Proc Natl Acad Sci U S A 99, 13222-7.

Bernard, C., Hirsch, J. C. and Ben-Ari, Y., (1999). Excitation and inhibition in temporal lobe epilepsy: a close encounter. Adv Neurol 79, 821-8.

Binnie, C. D., Van Emde Boas, W. and Wauquier, A., (1985). Geniculate spikes during epileptic seizures induced in dogs by pentylenetetrazol and bicuculline. Electroencephalogr Clin Neurophysiol 61, 40-9.

Blümcke, I., Hof, P. R., Morrison, J. H. and Celio, M. R., (1990). Distribution of parvalbumin immunoreactivity in the visual cortex of old world monkeys and humans. J Comp Neurol 301, 417-432.

Bouilleret, V., Schwaller, B., Schurmans, S., Celio, M. R. and Fritschy, J. M., (2000). Neurodegenerative and morphogenic changes in a mouse model of temporal lobe epilepsy do not depend on the expression of the calcium-binding proteins parvalbumin, calbindin, or calretinin. Neuroscience 97, 47-58.

Bracci, E., Vreugdenhil, M., Hack, S. P. and Jefferys, J. G., (1999). On the synchronizing mechanisms of tetanically induced hippocampal oscillations. J Neurosci 19, 8104-13.

Bush, P. C., Prince, D. A. and Miller, K. D., (1999). Increased pyramidal excitability and NMDA conductance can explain posttraumatic epileptogenesis without disinhibition: a model. J Neurophysiol 82, 1748-58.

Caillard, O., Moreno, H., Schwaller, B., Llano, I., Celio, M. R. and Marty, A., (2000). Role of the calcium-binding protein parvalbumin in short-term synaptic plasticity. Proc Natl Acad Sci U S A 97, 13372-7.

Cauli, B., Audinat, E., Lambolez, B., Angulo, M. C., Ropert, N., Tsuzuki, K., Hestrin, S. and Rossier, J., (1997). Molecular and physiological diversity of cortical nonpyramidal cells. J Neurosci 17, 3894-906.

Celio, M. R. and Blümcke, I., (1994). Perineuronal nets- a specialized form of extracellular matrix in the adult nervous system. Brain Res Rev 19, 128-145.

Celio, M. R. and Heizmann, C. W., (1982). Calcium-binding protein parvalbumin is associated with fast contracting muscle fibres. Nature 297, 504-6.

Celio, M. R., Spreafico, R., De Biasi, S. and Vitellaro-Zuccarello, L., (1998). Perineuronal nets: past and present. Trends Neurosci 21, 510-5.

Chagnac-Amitai, Y. and Connors, B. W., (1989). Synchronized excitation and inhibition driven by intrinsically bursting neurons in neocortex. J Neurophysiol 62, 1149-62.

Cohen, I., Navarro, V., Clemenceau, S., Baulac, M. and Miles, R., (2002). On the origin of interictal activity in human temporal lobe epilepsy in vitro. Science 298, 1418-21.

Congar, P., Leinekugel, X., Ben-Ari, Y. and Crepel, V., (1997). A long-lasting calcium-activated nonselective cationic current is generated by synaptic stimulation or exogenous activation of group I metabotropic glutamate receptors in CA1 pyramidal neurons. J Neurosci 17, 5366-79.

Cossart, R., Dinocourt, C., Hirsch, J. C., Merchan-Perez, A., De Felipe, J., Ben-Ari, Y., Esclapez, M. and Bernard, C., (2001). Dendritic but not somatic GABAergic inhibition is decreased in experimental epilepsy. Nat Neurosci 4, 52-62.

Davies, C. H. and Collingridge, G. L., (1993). The physiological regulation of synaptic inhibition by GABAB autoreceptors in rat hippocampus. J Physiol (Lond) 472, 245-65.

DeFelipe, J., (1997). Types of neurons, synaptic connections and chemical characteristics of cells immunoreactive for calbindin-D28K, parvalbumin and calretinin in the neocortex. J. Chem. Neuroanat. 14, 1-19.

DeFelipe, J., (1999). Chandelier cells and epilepsy. Brain 122, 1807-22.

DeFelipe, J., Garcia Sola, R., Marco, P., del Rio, M. R., Pulido, P. and Ramon y Cajal, S., (1993). Selective changes in the microorganization of the human epileptogenic neocortex revealed by parvalbumin immunoreactivity. Cereb Cortex 3, 39-48.

DeFelipe, J., Hendry, S. H. and Jones, E. G., (1989). Visualization of chandelier cell axons by parvalbumin immunoreactivity in monkey cerebral cortex. Proc Natl Acad Sci U S A 86, 2093-7.

Deisz, R. A., (2002). Cellular mechanisms of pharmacoresistance in slices from epilepsy surgery. Novartis Found Symp 243, 186-99.

Di Garbo, A., Barbi, M. and Chillemi, S., (2002). Synchronization in a network of fast-spiking interneurons. Biosystems 67, 45-53.

Diesmann, M., Gewaltig, M. O. and Aertsen, A., (1999). Stable propagation of synchronous spiking in cortical neural networks. Nature 402, 529-33.

Eisen, M. B. and Brown, P. O., (1999). DNA arrays for analysis of gene expression. Methods Enzymol 303, 179-205.

Engel, J., Jr., (1996). Excitation and inhibition in epilepsy. Can J Neurol Sci 23, 167-74.

Ferraro, T. N., Golden, G. T., Smith, G. G., St Jean, P., Schork, N. J., Mulholland, N., Ballas, C., Schill, J., Buono, R. J. and Berrettini, W. H., (1999). Mapping loci for pentylenetetrazol-induced seizure susceptibility in mice. J Neurosci 19, 6733-9.

Fujiwara-Tsukamoto, Y., Isomura, Y., Nambu, A. and Takada, M., (2003). Excitatory GABA input directly drives seizure-like rhythmic synchronization in mature hippocampal CA1 pyramidal cells. Neuroscience 119, 265-75.

Fukuda, T. and Kosaka, T., (2000). Gap junctions linking the dendritic network of GABAergic interneurons in the hippocampus. J Neurosci 20, 1519-28.

Gerlai, R., (1996). Gene-targeting studies of mammalian behavior: is it the mutation or the background genotype. Trends Neurosci 19, 177-181.

Hajos, N., Papp, E. C., Acsady, L., Levey, A. I. and Freund, T. F., (1998). Distinct interneuron types express m2 muscarinic receptor immunoreactivity on their dendrites or axon terminals in the hippocampus. Neuroscience 82, 355-76.

Hartley, D. M., Neve, R. L., Bryan, J., Ullrey, D. B., Bak, S. Y., Lang, P. and Geller, A. I., (1996). Expression of the calcium-binding protein, parvalbumin, in cultured cortical neurons using a HSV-1 vector system enhances NMDA neurotoxicity. Mol Brain Res 40, 285-296.

Haunso, A., Ibrahim, M., Bartsch, U., Letiembre, M., Celio, M. R. and Menoud, P., (2000). Morphology of perineuronal nets in tenascin-R and parvalbumin single and double knockout mice. Brain Res 864, 142-5.

Hefti, B. J. and Smith, P. H., (2000). Anatomy, physiology, and synaptic responses of rat layer V auditory cortical cells and effects of intracellular GABA(A) blockade. J Neurophysiol 83, 2626-38.

Hendrickson, A. E., Van Brederode, J. F., Mulligan, K. A. and Celio, M. R., (1991). Development of the calcium-binding protein parvalbumin and calbindin in monkey striate cortex. J Comp Neurol 307, 626-46.

Hendry, S. H., Jones, E. G., Emson, P. C., Lawson, D. E., Heizmann, C. W. and Streit, P., (1989). Two classes of cortical GABA neurons defined by differential calcium binding protein immunoreactivities. Exp Brain Res 76, 467-72.

Herrero, A. I., Del Olmo, N., Gonzalez-Escalada, J. R. and Solis, J. M., (2002). Two new actions of topiramate: inhibition of depolarizing GABA(A)- mediated responses and activation of a potassium conductance. Neuropharmacology 42, 210-20.

Hof, P. R., Glezer, II, Conde, F., Flagg, R. A., Rubin, M. B., Nimchinsky, E. A. and Vogt Weisenhorn, D. M., (1999). Cellular distribution of the calcium-binding proteins parvalbumin, calbindin, and calretinin in the neocortex of mammals: phylogenetic and developmental patterns. J Chem Neuroanat 16, 77-116.

Hooper, M., Hardy, K., Handyside, A., Hunter, S. and Monk, M., (1987). HPRT- deficient (Lesh-Nyhan) mouse embryos derived from germline colonization by cultured cells. Nature 326, 292-295.

Jones, E. G., (1993). GABAergic neurons and their role in cortical plasticity in primates. Cereb Cortex 3, 361-72.

Kaila, K., (1994). Ionic basis of GABAA receptor channel function in the nervous system. Prog Neurobiol 42, 489-537.

Kaila, K., Lamsa, K., Smirnov, S., Taira, T. and Voipio, J., (1997). Long-lasting GABA-mediated depolarization evoked by high-frequency stimulation in pyramidal neurons of rat hippocampal slice is attributable to a network-driven, bicarbonate-dependent K+ transient. J Neurosci 17, 7662-72.

Kawaguchi, Y. and Kubota, Y., (1993). Correlation of physiological subgroupings of nonpyramidal cells with parvalbumin- and calbindinD28k-immunorective neurons in layer V of rat frontal cortex. J. Neurophysiol. 70, 387-396.

Kawaguchi, Y. and Kubota, Y., (1997). GABAergic cell subtypes and their synaptic connections in rat frontal cortex. Cerebral Cortex 7, 476-486.

Kisvarday, Z. F., Kim, D. S., Eysel, U. T. and Bonhoeffer, T., (1994). Relationship between lateral inhibitory connections and the topography of the orientation map in cat visual cortex. Eur J Neurosci 6, 1619-32.

Klapstein, G. J., Vietla, S., Lieberman, D. N., Gray, P. A., Airaksinen, M. S., Thoenen, H., Meyer, M. and Mody, I., (1998). Calbindin-D28k fails to protect hippocampal neurons against ischemia in spite of its cytoplasmic calcium buffering properties: evidence from calbindin-D28k knockout mice. Neuroscience 85, 361-73.

Kohling, R., Vreugdenhil, M., Bracci, E. and Jefferys, J. G., (2000). Ictal epileptiform activity is facilitated by hippocampal GABAA receptor-mediated oscillations. J Neurosci 20, 6820-9.

Kosaka, T. and Heizmann, C. W., (1989). Selective staining of a population of parvalbumin-containing GABAergic neurons in the rat cerebral cortex by lectins with specific affinity for terminal N-acetylgalactosamine. Brain Res 483, 158-63.

Lambert, N. A., Harrison, N. L. and Teyler, T. J., (1991). Evidence for mu opiate receptors on inhibitory terminals in area CA1 of rat hippocampus. Neurosci Lett 124, 101-4.

Lambert, N. A. and Wilson, W. A., (1994). Temporally distinct mechanisms of use-dependent depression at inhibitory synapses in the rat hippocampus in vitro. J Neurophysiol 72, 121-30.

Lee, S. H., Rosenmund, C., Schwaller, B. and Neher, E., (2000a). Differences in Ca2+ buffering properties between excitatory and inhibitory hippocampal neurons from the rat. J. Physiol. (Lond.) 525, 405-418.

Lee, S. H., Schwaller, B. and Neher, E., (2000b). Kinetics of Ca2+ binding to parvalbumin in bovine chromaffin cells: implications for [Ca2+] transients of neuronal dendrites. J. Physiol. (Lond.) 525, 419-432.

Lewis, D. A. and Lund, J. S., (1990). Heterogeneity of chandelier neurons in monkey neocortex: corticotropin- releasing factor- and parvalbumin-immunoreactive populations. J Comp Neurol 293, 599-615.

Li, L. and Kelly, J. B., (1992). Binaural responses in rat inferior colliculus following kainic acid lesions of the superior olive: interaural intensity difference functions. Hear. Res. 61, 73-85.

Lopantsev, V. and Avoli, M., (1998). Participation of GABAA-mediated inhibition in ictallike discharges in the rat entorhinal cortex. J Neurophysiol 79, 352-60.

Loscher, W. and Nolting, B., (1991). The role of technical, biological and pharmacological factors in the laboratory evaluation of anticonvulsant drugs. IV. Protective indices. Epilepsy Res 9, 1-10.

Lüth, H.-J., Fischer, J. and Celio, M. R., (1992). Soybean lectin binding neurons in the visual cortex of the rat contain parvalbumin and are covered by glial nets. J. Neurocytol. 21, 211-221.

Lytton, W. W. and Sejnowski, T. J., (1991). Simulations of cortical pyramidal neurons synchronized by inhibitory interneurons. J Neurophysiol 66, 1059-79.

Marco, P., Sola, R. G., Pulido, P., Alijarde, M. T., Sanchez, A., Cajal, S. R. Y. and DeFelipe, J., (1996). Inhibitory neurons in the human epileptogenic temporal neocortex - An immunocytochemical study. Brain 119, 1327-1347.

Medvedev, A. V., (2002). Epileptiform spikes desynchronize and diminish fast (gamma) activity of the brain. An "anti-binding" mechanism? Brain Res Bull 58, 115-28.

Meier, T. J., Ho, D. Y. and Sapolsky, R. M., (1997). Increased expression of calbindin D-28k via herpes simplex virus amplicon vector decreases calcium ion mobilization and enhances neuronal survival after hypoglycemic challenge. J Neurochem 69, 1039-1047.

Mihaly, A., Szente, M., Dubravcsik, Z., Boda, B., Kiraly, E., Nagy, T. and Domonkos, A., (1997). Parvalbumin- and calbindin-containing neurons express c-fos protein in primary and secondary (mirror) epileptic foci of the rat neocortex. Brain Res 761, 135-145.

Mohler, H., Benke, D., Benson, J., Luscher, B. and Fritschy, J. M., (1995). GABAA-receptor subtypes in vivo: cellular localization, pharmacology and regulation. Adv Biochem Psychopharmacol 48, 41-56.

Oka, J. I., Kobayashi, T., Nagao, T., Hicks, T. P. and Fukuda, H., (1993). GABAA receptor-induced inhibition of neuronal burst firing is weak in rat somatosensory cortex. Neuroreport 4, 731-4.

Olsen, R. W., (1981). The GABA postsynaptic membrane receptor-ionophore complex. Site of action of convulsant and anticonvulsant drugs. Mol Cell Biochem 39, 261-79.

Otis, T. S., De Koninck, Y. and Mody, I., (1994). Lasting potentiation of inhibition is associated with an increased number of gamma-aminobutyric acid type A receptors activated during miniature inhibitory postsynaptic currents. Proc Natl Acad Sci U S A 91, 7698-702.

Perkel, D. H., Gerstein, G. L. and Moore, G. P., (1967a). Neuronal spike trains and stochastic point processes. I. The single spike train. Biophys J 7, 391-418.

Perkel, D. H., Gerstein, G. L. and Moore, G. P., (1967b). Neuronal spike trains and stochastic point processes. II. Simultaneous spike trains. Biophys J 7, 419-40.

Plogmann, D. and Celio, M. R., (1993). Intracellular concentration of parvalbumin in nerve cells. Brain Res. 600, 273-279.

Potier, M.-C., Gibelin, N., Cauli, B., Le Bourdelles, B., Lambolez, B., Golfier, G., Kuhlmann, S., Marc, P., Devaux, F. and Rossier, J. Developement of microarrays to study gene expression in tissue and single cells : analysis of neural transmission. In:,Microarrays for the Neurosciences: an essential guide. MIT Press, 2002: 237-254.

Prince, D. A., (1999). Epileptogenic neurons and circuits. Adv Neurol 79, 665-84.

Prince, D. A. and Jacobs, K., (1998). Inhibitory function in two models of chronic epileptogenesis. Epilepsy Res 32, 83-92.

Prince, D. A., Jacobs, K. M., Salin, P. A., Hoffman, S. and Parada, I., (1997). Chronic focal neocortical epileptogenesis: Does disinhibition play a role? Canadian J Physiol Pharmacol 75, 500-507.

Schena, M., Shalon, D., Davis, R. W. and Brown, P. O., (1995). Quantitative monitoring of gene expression patterns with a complementary DNA microarray. Science 270, 467-70.

Schierle, G. S., Gander, J. C., Dorlando, C., Celio, M. R. and Weisenhorn, D. M. V., (1997). Calretinin-immunoreactivity during postnatal development of the rat isocortex: A qualitative and quantitative study. Cereb Cortex 7, 130-142.

Schiffmann, S. N., Cheron, G., Lohof, A., d'Alcantara, P., Meyer, M., Parmentier, M. and Schurmans, S., (1999). Impaired motor coordination and purkinje cell excitability in mice lacking calretinin. Proc. Natl. Acad. Sci. U. S. A. 96, 5257-5262.

Schwaller, B., Buchwald, P., Blumcke, I., Celio, M. R. and Hunziker, W., (1993). Characterization of a polyclonal antiserum against the purified human recombinant calcium binding protein calretinin. Cell Calcium 14, 639-648.

Schwaller, B., Dick, J., Dhoot, G., Carroll, S., Vrbova, G., Nicotera, P., Pette, D., Wyss, A., Bluethmann, H., Hunziker, W., (1999). Prolonged contraction-relaxation cycle of fast-twitch muscles in parvalbumin knockout mice. Am J Physiol 276, C395-403.

Schwaller, B., Meyer, M. and Schiffmann, S. N., (2002). "New" functions for "old" proteins: The role of the calcium-binding proteins calbindin D-28k, calretinin and parvalbumin, in cerebellar physiology. Studies with knockout mice. The Cerebellum 1, 241-258.

Scotti, A. L., Kalt, G., Bollag, O. and Nitsch, C., (1997). Parvalbumin disappears from GABAergic CA1 neurons of the gerbil hippocampus with seizure onset while its presence persists in the perforant path. Brain Res 760, 109-117.

Solbach, S. and Celio, M. R., (1991). Ontogeny of the calcium binding protein parvalbumin in the rat nervous system. Anat. Embryol. 184, 103-124.

Somogyi, P., Tamas, G., Lujan, R. and Buhl, E. H., (1998). Salient features of synaptic organisation in the cerebral cortex. Brain Res Brain Res Rev 26, 113-35.

Soriano, E., Del Rio, J. A., Ferrer, I., Auladell, C., De Lecea, L. and Alcantara, S., (1992). Late appearance of parvalbumin-immunoreactive neurons in the rodent cerebral cortex does not follow an 'inside-out' sequence. Neurosci Lett 142, 147-50.

Stone, W. E. and Javid, M. J., (1979). Quantitative evaluation of the actions of anticonvulsants against different chemical convulsants. Arch Int Pharmacodyn Ther 240, 66-78.

Thomson, A. M., (1997). Activity-dependent properties of synaptic transmission at two classes of connections made by rat neocortical pyramidal axons in vitro. J Physiol (Lond) 502, 131-47.

Traub, R. D., Borck, C., Colling, S. B. and Jefferys, J. G., (1996). On the structure of ictal events in vitro. Epilepsia 37, 879-91.

Veliskova, J., Velisek, L. and Moshe, S. L., (1996). Age-specific effects of baclofen on pentylenetetrazol-induced seizures in developing rats. Epilepsia 37, 718-22.

Villa, A. E., (1990). Physiological differentiation within the auditory part of the thalamic reticular nucleus of the cat. Brain Res Brain Res Rev 15, 25-40.

Villa, A. E., Tetko, I. V., Hyland, B. and Najem, A., (1999). Spatiotemporal activity patterns of rat cortical neurons predict responses in a conditioned task. Proc Natl Acad Sci U S A 96, 1106-11.

Villa, A. E. P., Dutoit, P., Tetko, I. V., Hunziker, W., Celio, M. and Schwaller, B., 2000. Non-linear coupling of local field potentials across cortical sites in parvalbumin-deficient mice. In: Chaos in Brain? (Lehnertz K., Arnhold J., Grassberger P., Elger C. E. eds.) World Scientific Publishing Co. Pte. Ltd., Singapur, pp. 243-246

Vreugdenhil, M., Jefferys, J. G. R., Celio, M. R. and Schwaller, B., (2003). Parvalbumin-deficiency facilitates repetitive IPSCs and related inhibition-based gamma oscillations in the hippocampus. J. Neurophysiol. 89, 1414-1423.

Whittington, M. A., Traub, R. D. and Jefferys, J. G., (1995). Erosion of inhibition contributes to the progression of low magnesium bursts in rat hippocampal slices. J Physiol (Lond) 486, 723-34.

Willoughby, J. O., Fitzgibbon, S. P., Pope, K. J., Mackenzie, L., Medvedev, A. V., Clark, C. R., Davey, M. P. and Wilcox, R. A., (2003). Persistent abnormality detected in the non-ictal electroencephalogram in primary generalised epilepsy. J Neurol Neurosurg Psychiatry 74, 51-5.

Yonekawa, W. D., Kupferberg, H. J. and Woodbury, D. M., (1980). Relationship between pentylenetetrazol-induced seizures and brain pentylenetetrazol levels in mice. J Pharmacol Exp Ther 214, 589-93.

Zimmer, A., (1996). Gene targeting and behaviour: a genetic problem requires a genetic solution. Trends Neurosci. 19, 470.

Legends to Figures

Fig. 1. (**A**) **Genotyping of PV-KO mice by PCR.** Amplification of either PV exon 3 (151 bp, lower arrow) or part of the neo-cassette (188 bp, upper arrow) allows for the distinction between the WT (+) or mutated allele (-). Genotypes of the four mice analyzed are indicated. As marker (M), Std. V from Roche was used. (**B**) Western blot of soluble proteins extracted from forebrain and cerebellum of PV+/+, PV+/- or PV-/- mice using antibodies specific for parvalbumin (PV), calbindin D-28k (CB) or calretinin (CR). Total protein loads of forebrain and cerebellum proteins on gels were adapted to obtain similar staining intensities on Western blots: PV (60 µg and 10 µg), CB (20 µg and 5 µg) and CR (20 µg and 10 µg), respectively. Purified recombinant proteins (PV: 25 ng, CB: 40 ng, CR: 25 ng) were used as controls (co). On all three membranes one single protein of the correct size was recognized by each of the three antibodies and only the regions of interest are shown.

Fig. 2. Immunohistochemistry of 40 µm cryostat brain sections (temporal cortex) from the 3 genotypes stained with anitsera against PV, CB and CR. Perineuronal nets around PV-expressing neurons were stained with peroxidase-coupled isolectin B4 *Vicia Villosa* agglutinin (VVA). Scale bar for PV, CB and CR image: 500 µm; for VVA: 200 µm A) PV and VVA staining; B) CB and CR. Due to the thickness of the sections not all immunostained neurons are in the same focal plane.

Fig. 3 Relative levels of $GABA_A$(R) subunits in the forebrain determined by Western blot analysis. Representative Western blot signals for the GABA receptor subunits α2, α3 and β2/β3in PV+/+ and PV-/- mice. Semi-quantitative analysis of ECL signals (n = 3 animals for both genotypes) revealed no significant differences between PV+/+ and PV-/- samples.

Fig. 4 (**a**) **Seizure intensity of mice treated with convulsant doses of pentylenetetrazole (PTZ).** Seizure stages (defined in Material and Methods) were determined by injection of PTZ (60 or 70 mg/kg i.p.) for the 3 genotypes (mean ± S. E. M.). Significant differences between the three genotypes at 60 mg/kg PTZ is corroborated by a non-parametric Kruskal-Wallis test, which showed a p-value < 0.001.

* Significant vs. WT; $p < 0.001$ using the Mann-Whitney U-Test). **(b)** For experiments with 60 mg/kg PTZ (n=18 for PV+/+, n=19 for PV+/- and n=23 for PV-/-), the relative distribution of seizure stages were plotted. **(c) Latency of the onset of clonic-tonic seizures (CTS) as a function of PTZ dose injected for the 3 genotypes.** The lag period before onset is decreased with increasing doses of PTZ in all groups. PV-/- mice show a tendency to start CTS with a small delay compared to PV+/- or PV+/+ mice. At 60 mg/kg PTZ, a non-parametric Kruskal-Wallis test revealed significant differences between PV+/+, PV+/- and PV-/- with a p-value < 0.05. * Significant vs. PV+/+; $p < 0.01$ (Mann-Whitney U-Test).

Fig. 5. **Typical autocorrelograms (auto renewal density histograms) of the three types of spontaneous firing pattern observed in extracellular single unit recordings from the temporal cortex, with lag (ms) on the abscissa and rate (spikes/s) on the ordinate.** Note that abscissa is scaled to 500 ms and the ordinate is scaled to 9 spikes/s for all plots. The histograms are smoothed by a Gaussian bin of 10 ms. The average firing rate of the unit is indicated by the continuous line, whereas the broken lines correspond to 99% confidence limits following a Poisson distribution. Each autocorrelogram has an inset showing the oscilloscope traces of the corresponding extracellularly recorded single unit. (**a**) 'Regular' firing unit. (**b**) 'Irregular' firing unit. (**c**) Bursting' firing unit, characterized by burst duration larger than 80 ms and intra-burst frequency less than 30 Hz. (**d**) Distribution of electrophysiologically defined cell types in PV-/-, PV+/- and PV +/+ mice. Note that in PV -/- the proportion of “Regular” firing neurons was increased.

Fig. 6 Facilitated $GABA_A$ergic current reversal with high-frequency stimulation. A. The response of a CA1 hippocampal neuron from a PV+/+ mouse to tetanic stimulation (20 pulses at 100 Hz) at maximal IPSP stimulus intensity recorded in current clamp in standard solution, in the presence of the $GABA_A$ receptor antagonist bicuculline methiodide (BMI; 50 μM) and after addition of the metabotropic glutamate receptor group I antagonist (S)-3-carboxy-4-hydroxyphenylglycine (CPG; 50 μM). Tetanic stimulation evokes a late slow $GABA_A$ergic depolarization, triggering repetitive firing. The early $GABA_A$ergic hyperpolarisation masks a metabotropic glutamate receptor-mediated depolarization. **B.** Under voltage-clamp conditions tetanic stimulation causes a slow inward current following an outward current in standard

solution. Bicuculline (BMI; 50 μM) unmasks a small inward current that is restricted to the duration of the tetanic stimulus.

Tables

Table 1 Parvalbumin ELISA: values* in µg/mg of soluble protein

	Forebrain	Cerebellum	Kidney	TA	EDL
PV+/+	1,53	9,8	1,81	37,5	27,6
PV+/-	0,52	2,95	0,57	19,46	9
PV-/-	ø	ø	ø	ø	ø
% PV in PV+/- vs. PV+/+	34*	30	31	52	33

TA: Tibialis anterior; EDL: Extensor digitorum longus

* Mean of 2 animals per genotype

Ø: not detectable; [PV] < 25 ng / mg protein)

Table 2 Spontaneous activity parameters of cortical units grouped according to the temporal pattern of discharges (median, mean ± S.E.M.)

Type	genotype	N	Firing rate (spikes/s)	Average burst duration (ms)	Average burst size (spikes)	Intra-burst frequency (Hz)	Bursting index (Hz)
Regular							
	$PV^{+/+}$	79	0.7 (1.3±0.2)	10.0* (16.2±2.2)	--	--	--
	$PV^{+/-}$	92	0.9 (1.1±0.1)	10.0* (14.8±2.4)	--	--	--
	$PV^{-/-}$	151	0.9 (1.4±0.2)	10.0* (12.0±0.9)	--	--	--
Irregular							
	$PV^{+/+}$	76	0.5 (0.8±0.1)	30.0 (45.4±5.5)	1.3 (2.0±0.3)	40.9 (45.7±1.8)	0.8 (1.1±0.1)
	$PV^{+/-}$	140	0.6 (0.9±0.1)	30.0 (34.8±1.6)	1.4 (1.7±0.1)	50.6 (53.0±1.5)	0.7 (0.8±0.1)
	$PV^{-/-}$	84	0.8 (1.2±0.2)	30.0 (37.8±3.0)	1.3 (1.7±0.1)	42.5 (47.8±1.8)	0.8 (0.9±0.1)
Bursting							
	$PV^{+/+}$	199	0.8 (1.2±0.1)	90.0 (89.5±2.9)	1.5 (1.6±0.1)	18.6 (19.3±0.4)	4.5 (5.6±0.3)
	$PV^{+/-}$	165	1.0 (1.3±0.1)	95.0 (98.5±4.0)	1.6 (1.8±0.1)	19.1 (19.5±0.5)	4.6 (6.4±0.5)
	$PV^{-/-}$	132	1.1 (1.4±0.1)	90.0 (96.4±4.3)	1.4 (1.6±0.1)	18.6 (18.9±0.5)	4.8 (6.4±0.5)

* For the 'regular' firing units this duration corresponds to the refractory period.

Fig.1

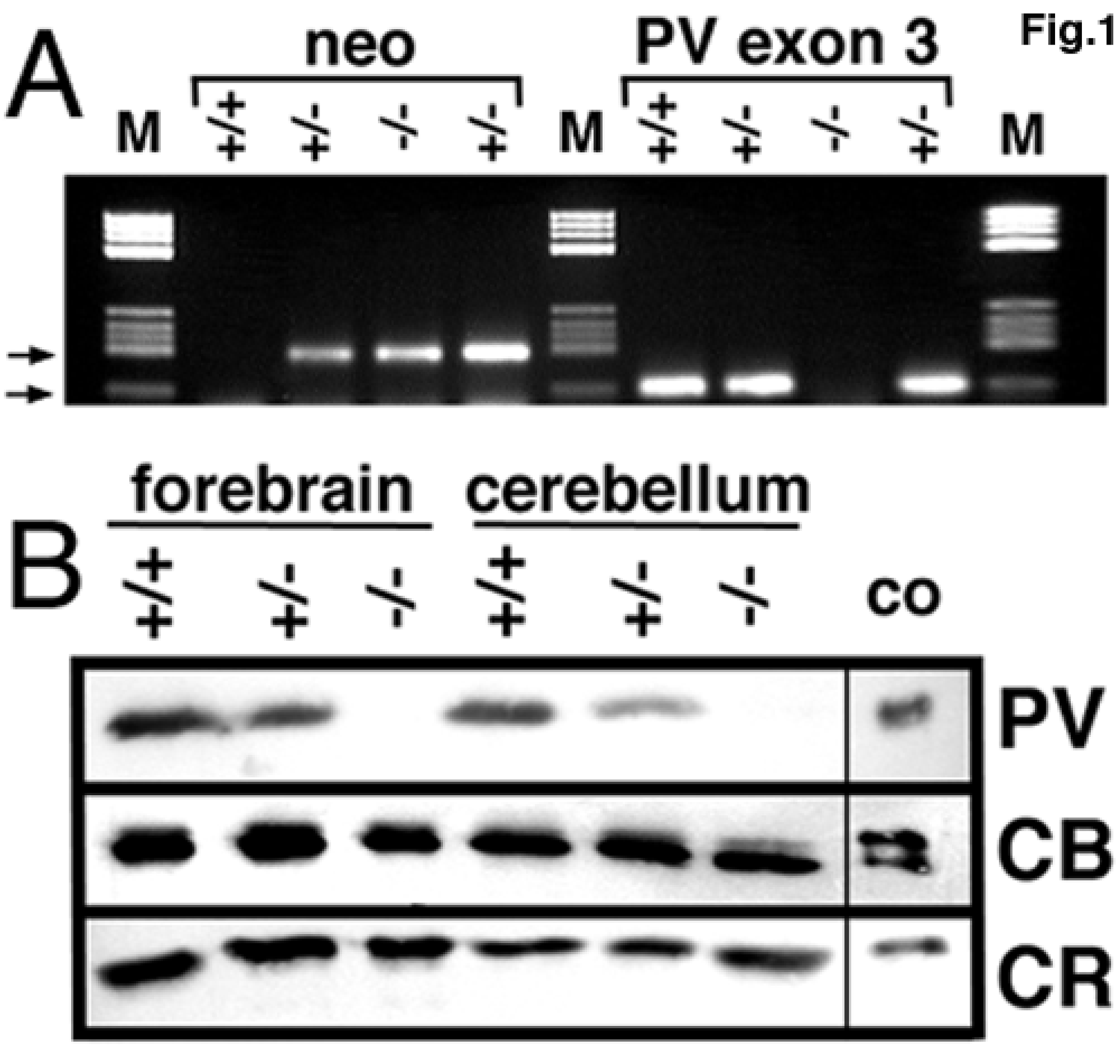

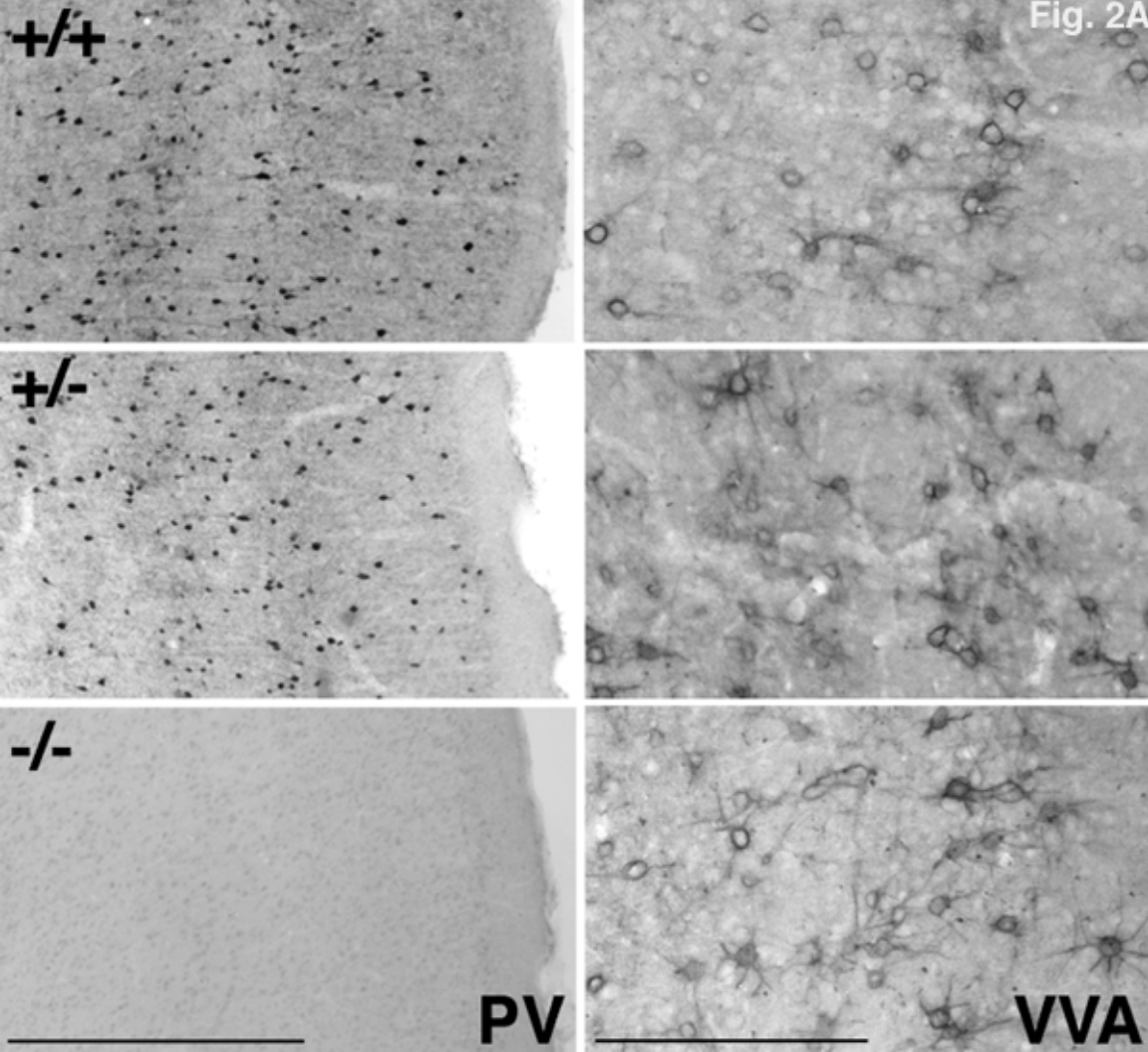

Fig. 2A

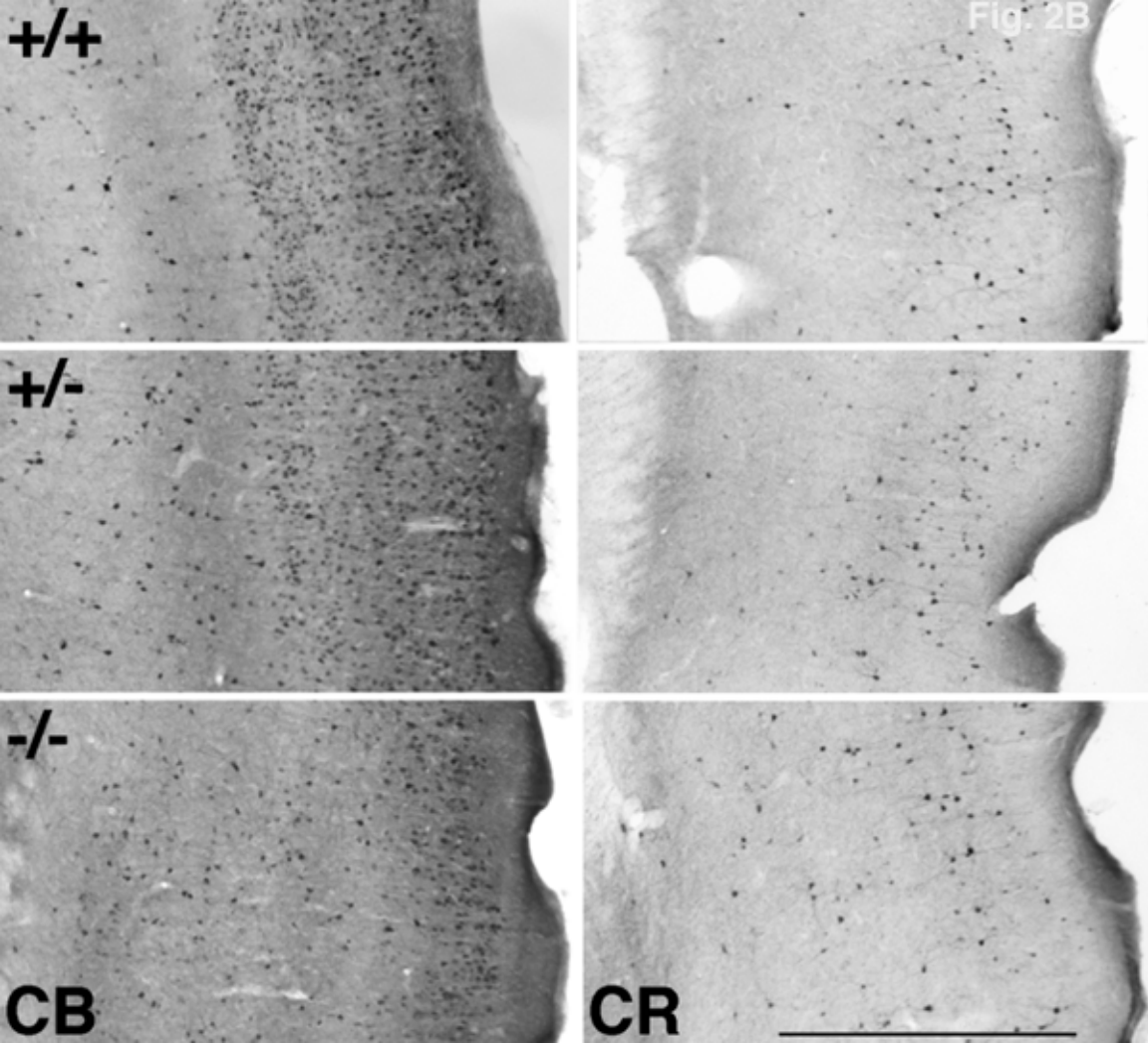
Fig. 2B
+/+
+/-
-/-
CB
CR

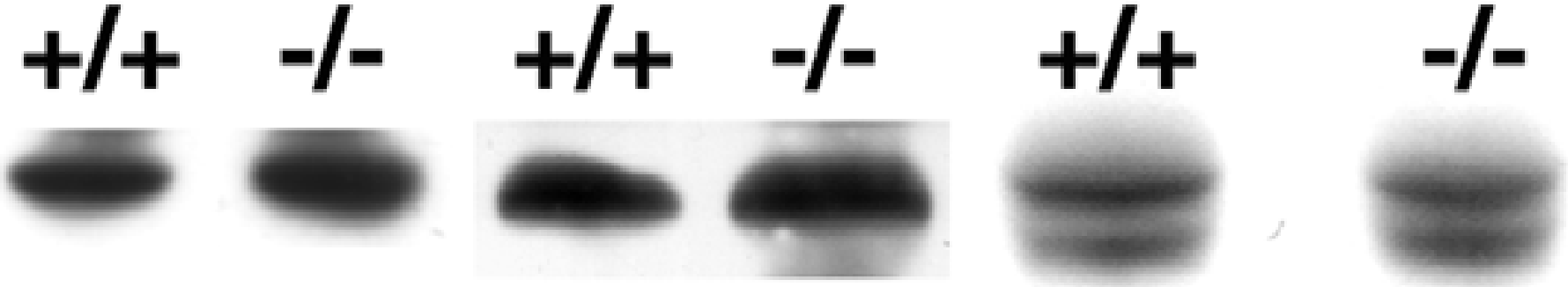

Fig. 3

Figure 4A

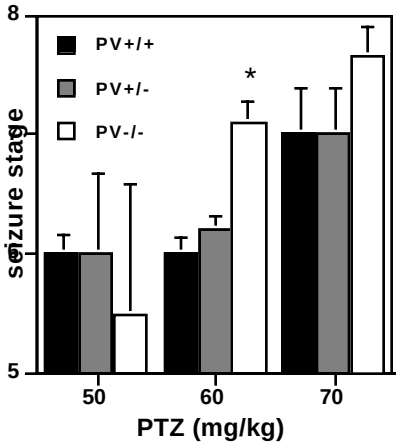

Figure 4B

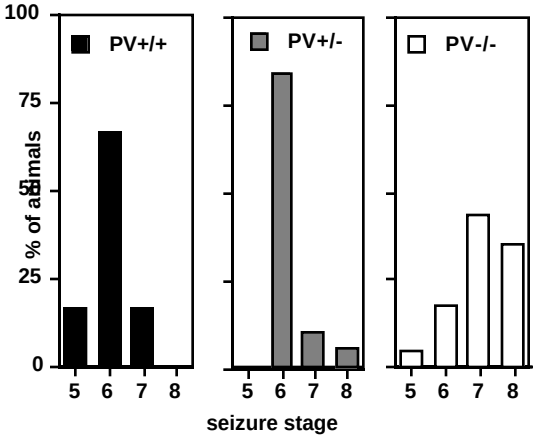

Figure 4C

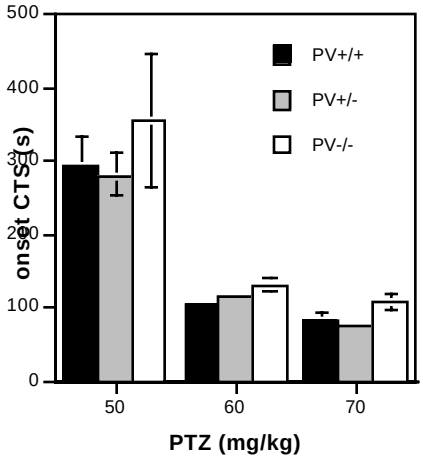

Fig. 5

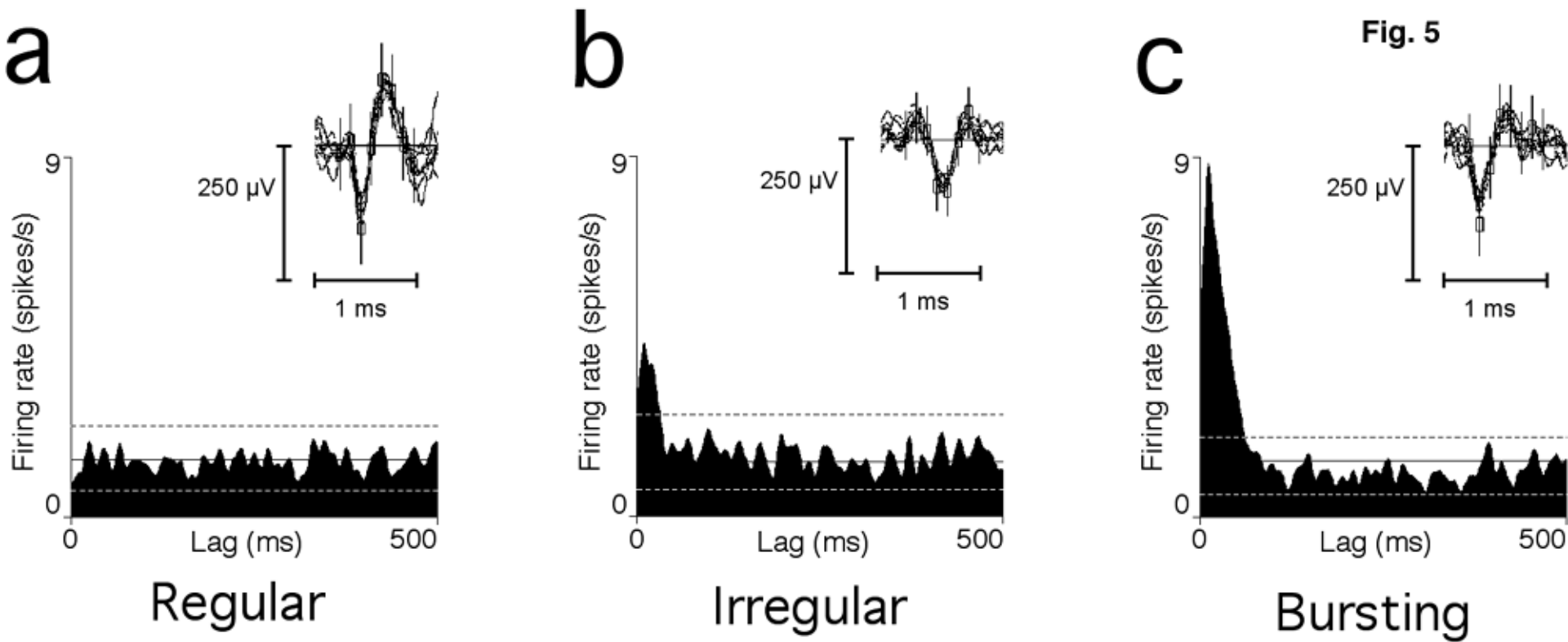
a
b
c
9
0
Firing rate (spikes/s)
250 µV
1 ms
0
Lag (ms)
500
Regular
Irregular
Bursting

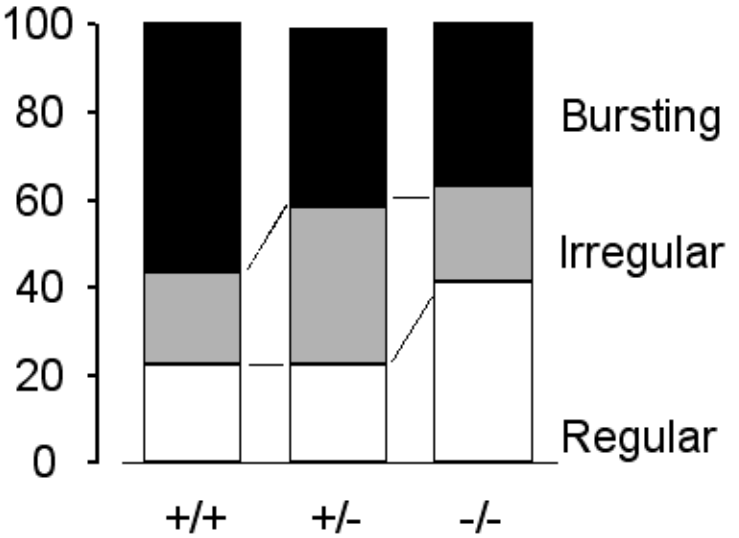

Fig.5D

Fig. 6